

# Geophysical Research Letters®



## RESEARCH LETTER

10.1029/2022GL102365

## Modeling the Intermittent Lava Lake Drops Occurring Between 2015 and 2021 at Nyiragongo Volcano

D. Walwer<sup>1</sup> , C. Wauthier<sup>1,2</sup> , J. Barrière<sup>3</sup> , D. Smittarello<sup>3</sup> , B. Smets<sup>4,5</sup>, and N. d'Oreye<sup>3,6</sup> 

### Key Points:

- Nyiragongo 2015–2021 successive lava lake level drops modeled as the result of ~15 km deep lateral transport of magma
- Nyiragongo's modeled central reservoir distributes the fluid up into the lava lake and laterally into a distal storage zone
- Lava lake overflows exert top-down control on magma transport phenomena occurring in the deeper part of the plumbing system

### Supporting Information:

Supporting Information may be found in the online version of this article.

### Correspondence to:

D. Walwer,  
[damianwalwer@gmail.com](mailto:damianwalwer@gmail.com)

### Citation:

Walwer, D., Wauthier, C., Barrière, J., Smittarello, D., Smets, B., & d'Oreye, N. (2023). Modeling the intermittent lava lake drops occurring between 2015 and 2021 at Nyiragongo volcano. *Geophysical Research Letters*, 50, e2022GL102365. <https://doi.org/10.1029/2022GL102365>

Received 2 DEC 2022  
Accepted 11 MAR 2023

<sup>1</sup>Department of Geosciences, Pennsylvania State University, University Park, PA, USA, <sup>2</sup>Institute for Computational and Data Sciences, Pennsylvania State University, University Park, PA, USA, <sup>3</sup>European Center for Geodynamics and Seismology (ECGS), Walferdange, Luxembourg, <sup>4</sup>Natural Hazards Service, Department of Earth Sciences, Royal Museum for Central Africa (RMCA), Tervuren, Belgium, <sup>5</sup>Cartography and GIS Research Group, Department of Geography, Vrije Universiteit Brussel, Brussels, Belgium, <sup>6</sup>Department of Geophysics/Astrophysics, National Museum of Natural History (NMNH), Luxembourg City, Luxembourg

**Abstract** Between 2015 and 2021, Nyiragongo's lava lake level experienced a linear increase punctuated by fast intermittent drops. These drops occurred synchronously to seismic swarm at approximately 15 km below the surface and extending laterally NE from the volcano. To interpret these lava lake level patterns in terms of reservoirs pressure evolution within Nyiragongo, we consider the following simplified plumbing system: a central reservoir is fed by a constant flux of magma, distributing the fluid up into the lava lake and laterally into a distal storage zone. Magma transport is driven by a pressure gradient between the magma storage bodies, accommodating influx and outflow of magma elastically, and the lava lake. Lateral transport at depth occurs through a hydraulic connection for which the flow resistance is coupled to the magma flux. When the right conditions are met, lateral magma transport occurs intermittently and triggers intermittent lava lake level drops matching the observations.

**Plain Language Summary** The level of lava lakes fluctuates in response to magma motion in the underlying crust. Prior to the May 2021 flank eruption, Nyiragongo's lava lake level displayed a series of rapid drops in concert with ~15 km deep earthquakes likely caused by crustal magma movements deforming and fracturing the surrounding rocks. The present work studies the simplified physics of magma motion at depth draining the lava lake. We show that a valve-like mechanism either preventing or enabling deep magma flow can cause successive lava lake level drops as observed between 2015 and 2021 at Nyiragongo.

## 1. Introduction

Persistent lava lakes correspond to volumes of circulating magma exposed to the atmosphere and emerging from the underlying magma plumbing system (e.g., Lev et al., 2019). Examples of volcanoes hosting an active lava lake include Erebus in Antarctica, Erta 'Ale in Ethiopia, and Nyiragongo in Democratic Republic of Congo (e.g., Lev et al., 2019; Oppenheimer & Kyle, 2008; Oppenheimer et al., 2004). Kīlauea Volcano (Hawaii) also hosts a lava lake at its summit which successfully provided constrains on the magma plumbing system's temporal evolution (e.g., Patrick, Orr, et al., 2019). Kīlauea's lava lake sometimes behave as a piezometer: lava lake height variations mirror fluid pressure variations in the underlying reservoir (Patrick et al., 2015). Although lava lakes may not always act as piezometers, they are recognized as a window of observation into the underlying plumbing system, offering opportunities to monitor active effusive volcanoes (Allard et al., 2016; Barrière et al., 2019; Harris et al., 1999; Lev et al., 2019; Patrick, Swanson, & Orr, 2019; Tazieff, 1994).

Nyiragongo Volcano in the East African Rift (EAR) hosts the largest known lava lake on Earth (e.g., Lev et al., 2019, and Figure 1a). The three most recent flank eruptions at Nyiragongo occurred in 1977, 2002, and 2021 (Figure 1b) (Komorowski et al., 2002; Smittarello et al., 2022; Tazieff, 1977). All three eruptions involved significant and rapid drainage of the lava lake (Komorowski et al., 2002; Tazieff, 1977; Wauthier et al., 2012). Together with the subsequent refilling, these events suggest an effective hydraulic connections between the lava lake and other parts of the plumbing system, as previously recognized (Tazieff, 1985).

Measurements of Nyiragongo's lava lake level started in the twentieth century and captured, although very sporadically, the temporal evolution of the lava lake level preceding to the 1977 eruption (Durieux, 2002; Le Guern, 1987). Recent lava lake level monitoring using remote sensing provides an increased temporal resolution and reveals

© 2023. The Authors.

This is an open access article under the terms of the [Creative Commons Attribution-NonCommercial-NoDerivs License](https://creativecommons.org/licenses/by-nc-nd/4.0/), which permits use and distribution in any medium, provided the original work is properly cited, the use is non-commercial and no modifications or adaptations are made.

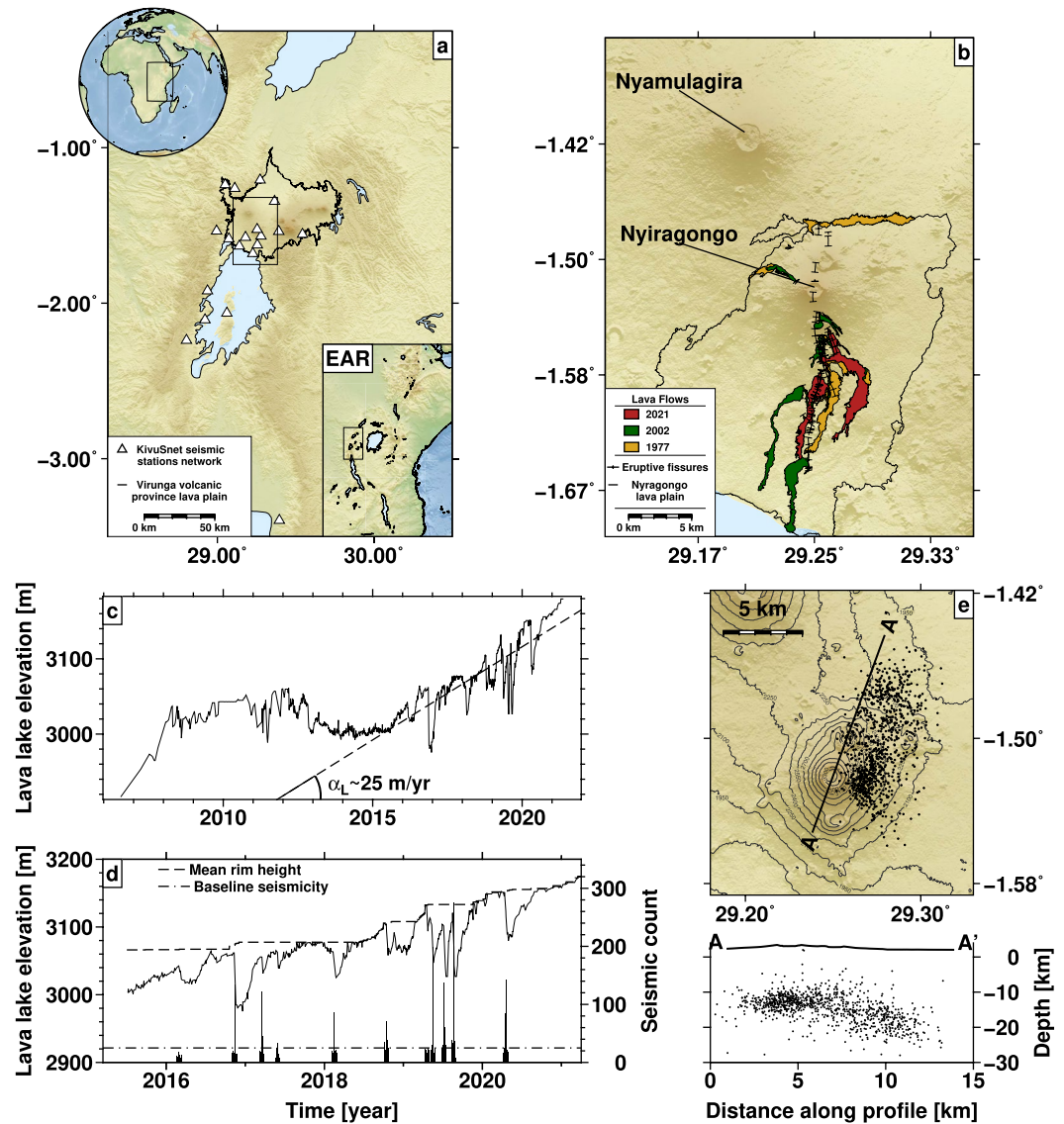


**Figure 1.** Nyiragongo geodynamic context and geophysical observations. (a) Map of the Lake Kivu region displaying the Virunga volcanic province lava field as well as seismic stations from the KivuSnet network. The black rectangular frames the map displayed on panel (b) and shows Nyiragongo location within the Virunga volcanic province. The top left inset locates the East African Rift displayed in the bottom right inset including a rectangular frame locating the Lake Kivu region. (b) Map centered on Nyiragongo. (c) Lava lake level time series from 2006 to 2021 from Barrière et al. (2022). (d) Zoom onto the 2015–2021 period displaying a linear level increase and drops superimposed onto it. Histograms represent seismic count during each drop often exceeding seismicity baseline. (e) Location of the seismic swarms synchronous to the lava lake level drops.

several interesting temporal patterns (Barrière et al., 2022). These new lava lake observations are often correlated with other geophysical signals and, in particular, with acoustic and seismic observations made possible by recent monitoring network development in the Kivu Rift Region (Barrière et al., 2018; Oth et al., 2017; Figure 1a).

Short duration (seconds to hours) and small amplitude lava lake fluctuations are often correlated with the occurrence of shallow low-frequency earthquakes and attributed to shallow gas-driven processes such as a gas-piston phenomenon (e.g., Barrière et al., 2019; Patrick et al., 2016; Smets et al., 2017). Conversely, intermittent or continuous increases in lava lake level over years likely reflect magma supply from the mantle recharging crustal reservoirs (e.g., Burgi et al., 2014; Patrick, Orr, et al., 2019). In between those two end-members in duration and amplitude, lie other interesting phenomena such as successive rapid drops (minutes to days) and subsequent

slow refilling (weeks to months). At Nyiragongo, these drops, unrelated to a flank eruption, have been observed sparsely before 2015 (e.g., Barrière et al., 2019; Bobrowski et al., 2017). In between 2015 and 2021, the drops punctuate the secular linear increase of lava lake level preceding the May 2021 eruption (Barrière et al., 2022). They are associated with seismic swarms located much deeper (10–20 km deep) than the shallow low-frequency seismicity related to the lava lake spattering activity (Barrière et al., 2018, 2019). Studying these patterns, together with modeling physical interactions between the lava lake and magmatic reservoirs, help to understand the lava lake's response to change in pressure occurring within Nyiragongo's magma plumbing system. They also offer the opportunity to constrain further Nyiragongo's magmatic evolution leading to the May 2021 eruption (Montgomery-Brown, 2022; Smittarello et al., 2022).

The present study has two purposes: (a) presenting a simple physics-based modeling framework to understand under which conditions deep lateral magma transport causes the lava lake drops at Nyiragongo between 2015 and 2021 and (b) to propose a mechanism that accounts for the apparent periodicity of the observed lava lake level drops.

## 2. 2015–2021: Lava Lake Level Drops and Synchronous Seismic Activity

This work is based on recent observations of Nyiragongo's volcanic and magmatic activity gathered by Barrière et al. (2022) and summarized in Figures 1c–1e. We exploit in particular the updated time series of Nyiragongo's lava lake level displayed in Figure 1d to mine for information about Nyiragongo's magma plumbing system dynamics. The time series was obtained by combining dense lava lake and crater floor elevation measurements from radar satellite images validated by punctual photogrammetry field measurements (Barrière et al., 2018, 2022). Its higher accuracy and temporal resolution during the recent period contrasts with other recently published time series based on much fewer, in situ only, measurements (Burgi et al., 2020).

The time series presented in Figure 1c starts in May 2006 and ends in May 2021. It displays an overall long term increase of lava lake level from 2006 to 2021 interrupted by a period of decrease between 2012 and 2015. It is followed by a period of overall linear increase in lava lake level of ~25 m/yr from 2015 to 2021 (gray line in Figure 1a). Fluctuations of various periods and amplitudes are superimposed onto the long period trends of variability described above. In particular, the rapid lava lake level drops occurring in apparent cyclicity are superimposed onto the overall linear increase preceding the 2021 eruption (Figure 1d).

Most of the observed lava lake drops occur synchronously with increase in seismicity located  $\geq 10$  km below the surface (Figures 1d and 1e, Barrière et al., 2019, 2022). The depth of this seismicity correlates with magma bodies inferred from seismological and petrological data sets (Barrière et al., 2022; Demant et al., 1994; Tanaka, 1983). The seismicity is made of “hybrid” events sharing characteristics with both volcano-tectonic and long period earthquakes (Barrière et al., 2019). They form swarms extending NE of Nyiragongo, following the local rift direction (Figure 1e). Earthquake count peaks during the drops of the lava lake and comes back to baseline level within ~3 days (Barrière et al., 2018, 2022).

## 3. Interactions Between the Lava Lake and the Magma Plumbing System

### 3.1. Model Set-Up

Our approach is based on macroscopic magma volume conservation within the magma plumbing system (e.g., Pinel et al., 2010; Reverso et al., 2014; Wang et al., 2021). While previously published dynamical models of Nyiragongo's lava lake attempted to investigate its interaction with a shallow reservoir (Burgi et al., 2014, 2018, 2020), our model focuses on investigating the interactions between the lava lake and deeper parts of Nyiragongo's magma plumbing system. Our goal is to define under which conditions the successive level drops and synchronous deep seismicity can be caused by deep lateral magma transport rather than shallower magmatic processes. The simplified magma plumbing system, schematized in Figure 2a, includes: a deep central reservoir fed by a constant flux of magma  $Q$  distributing the magma upward into the lava lake or laterally into a distal storage zone.

The rate of magma volume variation within each compartment is equal to the differences between magma influx and outflux:

$$\frac{dV_L}{dt} = q_{RL} \quad (1a)$$

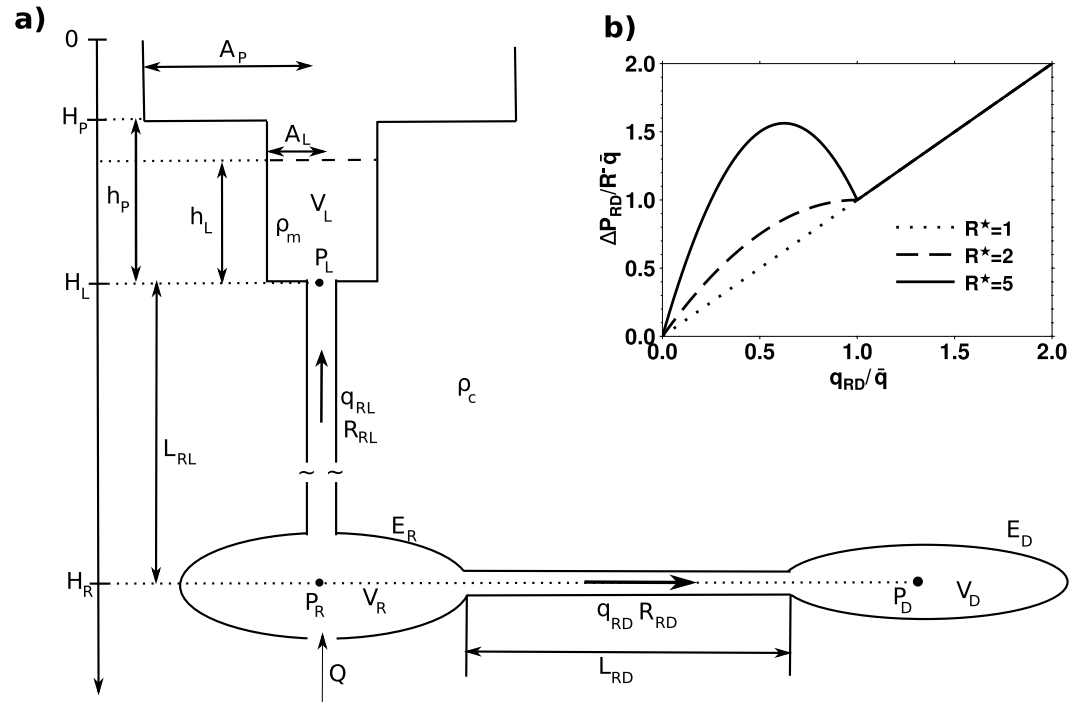


**Figure 2.** Model set up. (a) Schematic of the simplified magma plumbing system at Nyiragongo including key variables and parameters (summarized in Tables S1 and S2 in Supporting Information S1). A central reservoir located at depth  $H_R$  is fed by a constant flux of magma  $Q$  distributed up into the lava lake and laterally into a distal storage zone. The lava lake is considered as a cylinder of cross sectional  $A_L$  and has a level equal to  $h_L$ . When the lava lake overflows it fills the cylinder of cross sectional  $A_P$  formed by the surrounding platform. (b) Pressure flow-curve pertaining to magma transport from the central reservoir into the distal storage zone relating the pressure difference  $\Delta P_{RD}$  to the flux  $q_{RD}$ . As the value of  $R^* = R^*/R^*$  increases and surpasses 2, the flow-pressure curve becomes non-monotonous allowing for unstable flow behavior which induces intermittent episodes of lateral magma transport.

$$\frac{dV_R}{dt} = Q - q_{RL} - q_{RD} \quad (1b)$$

$$\frac{dV_D}{dt} = q_{RD}. \quad (1c)$$

The volume within the central reservoir, the lava lake, and the distal storage zone is  $V_R$ ,  $V_L$ , and  $V_D$ , respectively.  $q_{RL}$  is the volumetric flux of magma leaving the central reservoir into the lava lake and  $q_{RD}$  is the volumetric flux of magma leaving the central reservoir into the distal storage zone. All variables and parameters are summarized in Tables S1 and S2 in Supporting Information S1.

### 3.2. Relationships Between Pressure and Volume Within the Lava Lake, the Central Reservoir, and the Distal Storage Zone

The relationship between lava lake volume and elevation  $h_L(t)$  depends on the lava lake geometry. Recent observations show that the upper part of the lava lake is approximately cylindrical during the period we aim at modeling (see Figure 5 in Barrière et al., 2022). Accounting also for magma overflowing, the lava lake volume and height are related as follow:

$$V_L(t) = A_L h_L(t) \quad 0 \leq h_L(t) \leq h_P(t) \quad (2a)$$

$$V_L(t) = A_L h_P(t) + A_P (h_L(t) - h_P(t)) \quad h_L(t) > h_P(t) \quad (2b)$$

where  $A_L$  is the lava lake cross sectional area and  $h_P(t)$  is the elevation of the surrounding platform. When  $h_L > h_P$ , the lava lake overflows and the lava fills up the larger cylinder formed by the platform of circular cross

sectional area  $A_p$  surrounding the lava lake (Figure 2a). The pressure  $P_L$  at the base of the lava lake is considered magmastic:

$$P_L = \rho_m g h_L \quad (3)$$

where  $\rho_m$  is the magma density and  $g$  the acceleration of gravity.

Assuming that the central reservoir and distal storage zone accommodate change in volume elastically, the change in fluid pressure is:

$$\Delta P_R = E_R \frac{\Delta V_R}{V_R} \quad (4a)$$

$$\Delta P_D = E_D \frac{\Delta V_D}{V_D} \quad (4b)$$

where  $E_R$  and  $E_D$  are the effective bulk modulus of the central reservoir and the distal storage zone, respectively (e.g., Huppert & Woods, 2002).

### 3.3. Relationship Between Magma Volumetric Flux and Fluid Pressure

#### 3.3.1. Magma Flux Between the Reservoir and the Lava Lake

Magma transport is driven by the fluid pressure gradient across the plumbing system. Following common practice, we assume an Hagen-Poiseuille flow between the central reservoir and the lava lake (e.g., pp. 180–181 of Batchelor and Batchelor (2000), Pinel et al. (2010), Reverso et al. (2014), Wang et al. (2021)). It implies that:

$$q_{RL} = \frac{1}{R_{RL}} (P_R - P_L - \rho_m g L_{RL}) \quad (5)$$

where  $P_R$  and  $P_L$  is the fluid pressure within the reservoir and the lava lake, respectively.  $L_{RL}$  is the length of the conduit between the reservoir and the lava lake. The flow resistance  $R_{RL}$  simply relates the pressure difference to the fluid flux.

It is convenient to express the fluid pressure in the reservoir as the sum of the lithostatic pressure exerted by the host rock onto the reservoir and an overpressure, that is,  $P_R = \rho_c g H_R + \Delta P_R$ ;  $\rho_c$  being the rock density and  $H_R$  the reservoir depth. Similarly, we can express the pressure at the base of the lava lake as a sum of a reference pressure and an overpressure so  $P_L = \rho_m g H_L + \Delta P_L$ . The reference pressure  $\rho_m g H_L$  is the magmastic pressure at the base of the lava lake if entirely filled. In that case:

$$q_{RL} = \frac{1}{R_{RL}} (\Delta P_R - \Delta P_L + \Delta \rho g H_R) \quad (6)$$

where  $\Delta \rho = \rho_c - \rho_m$  and  $H_R = H_L + L_{RL}$ . It shows that the magma flux  $q_{RL}$  is driven by fluid overpressure difference between the reservoir and the lava lake as well as magma buoyancy  $\Delta \rho g H_R$ .

Importantly, injecting Equations 6 and 2 into Equations 1a provides

$$\frac{dh_L}{dt} = \frac{1}{R_{RL}} (\Delta P_R - \Delta P_L + \Delta \rho g H_R) \times \frac{1}{A_{L,P}} \quad (7)$$

and shows how the lava lake's temporal evolution may depend on pressure within the plumbing system. Equation 7 is used to produce simulations of lava lake height  $h_L$  that are compared to the observed lava lake level displayed in Figure 1d. When the lake overflows, the lava fills a cylindrical volume of cross sectional area that increases from  $A_{L,P} = A_L$  to  $A_{L,P} = A_p$ . Overflows affect therefore the rate at which  $h_L$  changes and, as demonstrated in Section 3, can exert top-down control on magma transport phenomena occurring deeper in the plumbing system. As supported by the observed lava lake's rim height evolution displayed in Figure 1d, we further consider that overflows build up the surrounding platform, that is,  $dh_p/dt = dh_L/dt$  when  $h_L > h_p$  and that  $dh_p/dt = 0$  otherwise.

### 3.3.2. Flux Between the Reservoir and the Distal Storage Zone

Our model aims at explaining the occurrence of successive drops separated by phases of slower increase of lava lake level from 2015 to 2021 (Section 2). Such an asymmetric cyclic behavior can be accounted for by models possessing nonlinear oscillatory regimes called relaxation-oscillations (e.g., Jordan & Smith, 2007; Van der Pol, 1926; Walwer et al., 2022). For systems involving fluid flows in general and magma in particular, they may arise when the flow resistance is coupled to the volumetric flux (e.g., Barmin et al., 2002; Conrad, 1969; Melnik & Sparks, 1999; Pedley, 1980; Walwer et al., 2022; Whitehead & Helfrich, 1991).

We assume that the flow resistance  $R_{RD}$  pertaining to magma transport from the central reservoir to the distal storage zone depends on a length scale  $\bar{L}$  in such a way that:

$$R_{RD} = R^- \frac{\bar{L}}{L_{RD}} + R^+ \left(1 - \frac{\bar{L}}{L_{RD}}\right). \quad (8)$$

In other words, the total resistance  $R_{RD}$  connecting the pressure difference  $\Delta P_{RD} = P_R - P_D$  to the flux  $q_{RD}$ , is expressed as a function of local flow resistances that follow a step function increasing from  $R^-$  to  $R^+$  at distance  $\bar{L} \leq L_{RD}$  from the central reservoir (Figure 2a). Such a phenomenon occurs, for example, if the magma cools down and crystallizes along the path connecting the two compartments inducing an increase in local flow resistance from  $R^-$  to  $R^+$  caused by temperature-induced change in viscosity (Delaney & Pollard, 1982; Walwer et al., 2019; Whitehead & Helfrich, 1991).

We also assume that the distance  $\bar{L}$  is proportional to the flux  $q_{RD}$  and that the resistance can be expressed as a function of the flux  $q_{RD}$ :

$$R_{RD} = R^- \frac{q_{RD}}{\bar{q}} + R^+ \left(1 - \frac{q_{RD}}{\bar{q}}\right) \quad (9)$$

where  $\bar{q}$  is the value of the flux  $q_{RD}$  for which  $\bar{L} = L_{RD}$ . The resulting steady-state relationship between the discharge rate into the distal storage zone and the pressure difference  $\Delta P_{RD}$  expresses:

$$\Delta P_{RD} = \begin{cases} (R^- - R^+) \frac{q_{RD}^2}{\bar{q}} + R^+ q_{RD} & q_{RD} < \bar{q} \\ R^- q_{RD} & q_{RD} \geq \bar{q} \end{cases} \quad (10)$$

Corresponding flow-pressure curves are displayed in Figure 2b for different values of  $R^* = R^+/R^-$ .

An important property emerging from the flow-pressure relationship Equation 10 is the possibility for the curve to be non-monotonic, that is, a decrease in flux  $q_{RD}$  can be associated with an increase in  $\Delta P_{RD}$ . To account for the temporal manifestation of the flow instability that may arise in this situation, we allow the magma flow to accelerate and introduce the averaged momentum equation:

$$M \frac{dq_{RD}}{dt} = \begin{cases} \left( \Delta P_{RD} - (R^- - R^+) \frac{q_{RD}^2}{\bar{q}} - R^+ q_{RD} \right) & q_{RD} < \bar{q} \\ \Delta P_{RD} - R^- q_{RD} & q_{RD} \geq \bar{q} \end{cases} \quad (11)$$

where  $M$  can be referred to as the hydraulic inertance characterizing the flow from the central reservoir to the distal storage zone.  $M$  depends on the cross-sectional area  $A_{RD}$  of the pathway connecting the two storage zones and expresses  $M = \rho_m L_{RD} / A_{RD}$  in a case of a cylindrical conduit (Melnik & Sparks, 1999; Schönfeld, 1954; Walwer et al., 2019; Whitehead & Helfrich, 1991).

### 3.4. Set of Equations Governing the Plumbing System Evolution

Combining the set of Equation 1 expressing volume conservation within the plumbing system with relations linking pressure and volume in the lava lake, central reservoir, and the distal storage zone (Section 3.2), as well as with the expressions for the flux  $q_{RL}$  and  $q_{RD}$  (Section 3.3), provides the following set of ordinary differential equations (ODEs).

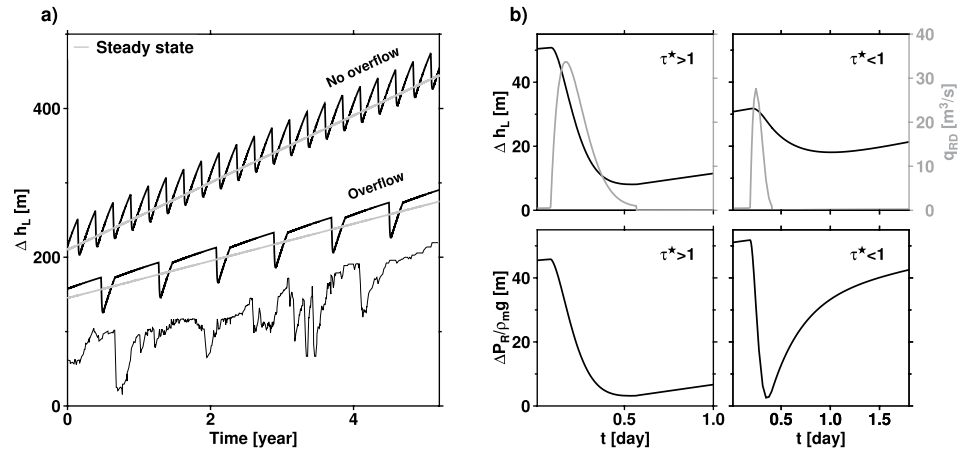


**Figure 3.** Model's results. (a) Simulated time series of lava lake level displaying successive rapid drops spaced by longer phase of increase (black lines) and the steady state evolution (gray line). Lava lake level drops are triggered by intermittent lateral magma transport. Top time series corresponds to a simulation without accounting for overflow while the middle time series accounts for overflows when  $h_L(t) > h_p(t)$ . For comparison the recorded lava lake level is displayed as the bottom time series. (b) Relationship between lava lake level drop, transient increase and decrease of  $q_{RD}$  and pressure drop in the central reservoir. Left panels display a piezometer-like lava lake ( $\tau^* > 1$ ) and the lava lake level mirrors the change of pressure  $\Delta P_R$ . Right panels display pressure difference between the lava lake and the central reservoir balances out with a delay with respect to the temporal evolution of the flux into the distal storage zone.

$$\frac{d\Delta P_{RL}}{dt} = \frac{E_R}{V_R} Q - \frac{1}{R_{RL}} \left( \frac{E_R}{V_R} + \frac{\rho_m g}{A_{L,P}} \right) (\Delta P_{RL} + \Delta \rho g H_R) - q_{RD} \frac{E_R}{V_R} \quad (12a)$$

$$\frac{d\Delta P_{RD}}{dt} = \frac{E_R}{V_R} Q - \left( \frac{E_R}{V_R R_{RL}} \right) (\Delta P_{RL} + \Delta \rho g H_R) - q_{RD} \left( \frac{E_R}{V_R} + \frac{E_D}{V_D} \right) \quad (12b)$$

$$\frac{dq_{RD}}{dt} = \begin{cases} \frac{1}{M} \left( \Delta P_{RD} - (R^- - R^+) \frac{q_{RD}^2}{\bar{q}} - R^+ q_{RD} \right) & q_{RD} < \bar{q} \\ \frac{1}{M} (\Delta P_{RD} - R^- q_{RD}) & q_{RD} \geq \bar{q} \end{cases} \quad (12c)$$

that govern pressure evolution within the magma plumbing system schematized in Figure 2a. The three main independent variables in the equation system Equation 12 are  $\Delta P_{RL} = \Delta P_R - \Delta P_L$ ,  $\Delta P_{RD} = \Delta P_R - \Delta P_D$ , and  $q_{RD}$ .

This set of ODEs can be solved numerically and is coupled with Equation 7 governing lava lake height to simulate time series of lava lake elevation that are compared with the observations as in Figure 3a. It shows that the modeled lava lake level time series capture, at first order, the main observed patterns of the lava lake level temporal evolution: successive lava lake level drops superimposed on a linear increase in elevation. In Section 4, we exposed our model's implications for understanding Nyiragongo's plumbing system dynamics during the period starting in 2015 and preceding the May 2021 eruption.

## 4. Insights From the Model

### 4.1. Steady State and Linear Increase in Lava Lake Elevation

A first insight is provided by studying the system equilibrium defined by  $d\Delta P_{RL}/dt = d\Delta P_{RD}/dt = dq_{RD}/dt = 0$ . It provides an expression for the steady state evolution of  $h_L$  and denoted  $h_L^0$  (see Section S2 in Supporting Information S1 for details):

$$h_L^0(t) = \left( 1 + \frac{V_D \rho_m g}{E_D A_{L,P}} + \frac{V_R \rho_m g}{E_R A_{L,P}} \right)^{-1} \frac{Q}{A_{L,P}} t. \quad (13)$$

It shows that when the flux  $Q$  feeding the central reservoir is constant, the lava lake level  $h_L(t)$  follows a linear evolution at a rate  $\alpha_L$  which depends on the storage capacities of the plumbing system. The term  $\left[1 + (V_D \rho_m g)/(E_D A_{L,P}) + (V_R \rho_m g)/(E_R A_{L,P})\right]$  in Equation 13 expresses the steady state portion of magma entering the system that goes into the lava lake and contributes to its filling instead of being stored in the central reservoir and the distal storage zone. The rate higher bound,  $Q/A_{L,P}$ , corresponds to the limit case where no magma is stored within the plumbing system, that is, all the magma from the source ends up into the lava lake. The gray lines in Figure 3a represent the steady state linear increase in  $h_L(t)$  obtained using expression Equation 13. It shows that even when the system oscillates and produces periodic lava lake drops, as displayed by the black line on Figure 3a, the long term variation of lava lake level follows the trend provided by its steady state expression Equation 13.

#### 4.2. Condition for a Piezometer-Like Lava Lake

Two important time scales can be extracted from the set of Equation 12. The study of the dynamical interaction between the reservoir and the lava lake provides a characteristic time:

$$\tau_{RL} = R_{RL} \left( \frac{E_R}{V_R} + \frac{\rho_m g}{A_L} \right)^{-1} \quad (14)$$

that governs the transient behavior emerging when a pressure difference is imposed between the lava lake and the central reservoir. Similarly, the hydraulic connection between the reservoir and the distal storage zone is characterized by the time scale:

$$\tau_{RD} = R^- \left( \frac{E_R}{V_R} + \frac{E_D}{V_D} \right)^{-1} \quad (15)$$

governing the duration of the transient behavior balancing the pressure between the two compartments (e.g., Pinel et al., 2010; Reverso et al., 2014; Walwer et al., 2019).

The lava lake dynamics depends significantly on the ratio  $\tau^* = \tau_{RD}/\tau_{RL}$  between these two time scales. The ratio  $\tau^*$  quantifies the relative efficiency of the two hydraulic connections in balancing out fluid pressure within the plumbing system. Effects of the value of  $\tau^*$  has on the lava lake dynamics are shown in Figure 3b. When  $\tau^* > 1$ , the lava lake response to changes in reservoir pressure induced by episodes of magma transport into the distal storage zone can be considered instantaneous. In this situation, the lava lake simply mirrors the history of the pressure drop occurring in the central reservoir and acts as a piezometer (Left panels of Figure 3b).

Conversely, when  $\tau^* < 1$ , the lava lake responds with a delay to change in  $\Delta P_R$  induced by magma acceleration and the value of  $q_{RD}$  peaks before the lava lake level significantly drops (right panels of Figure 3b). Everything else being equal, the resulting amplitude of the lava lake drop may also be lowered compared to the case  $\tau^* > 1$ : as the lava lake level slowly drops, pressure in the central reservoir is being rebuilt up due to magma supply  $Q$  from the source.

#### 4.3. Instability, Periodic Lateral Magma Transport, and Lava Lake Level Drop

In the following Subsection, we constrain ourselves to the case  $\tau^* > 1$ . Infrasound and seismic observations during large lava lake drops suggest no delay between deep and shallow magmatic processes in agreement with a piezometer-like behavior at Nyiragongo (Barrière et al., 2018). It simplifies the analysis of system Equation 12 while still providing insightful expressions informing the conditions for the successive lava lake drop to occur. Details on the derivation of the following expressions are provided in Supporting Information S1.

##### 4.3.1. Conditions for Intermittent Lateral Magma Transport

The emergence of an oscillatory regime characterized by intermittent magma transport into the distal storage zone is directly associated with the stability loss of system Equation 12's equilibrium point. It occurs when the

change in local flow resistance from  $R^-$  to  $R^+$  is high enough that the steady state flow-pressure curve becomes non monotonous. This transition occurs when:

$$R^* = \frac{R^+}{R^-} > 2 \quad (16)$$

as illustrated in Figure 2b where the curves for  $R^* \leq 2$  are monotonous while the curve for  $R^* > 2$  are not. Also, the equilibrium point is unstable only when the steady state value of  $q_{RD}$  is inferior to  $\bar{q}$  in such a way that the steady state relationship between  $\Delta P_{RD}$  and  $q_{RD}$  is characterized by varying flow resistance (Equation 10). It implies that:

$$\left(1 + \frac{V_R E_D}{E_R V_D} + \frac{A_{L,P} g E_D}{V_D \rho_m g}\right) > \frac{Q}{\bar{q}} > \frac{R^*}{2(R^* - 1)} \left(1 + \frac{V_R E_D}{E_R V_D} + \frac{A_{L,P} g E_D}{V_D \rho_m g}\right) \quad (17)$$

providing a condition for instability that depends on  $Q$ . When conditions Equations 17 and 16 are met, system Equation 12 exhibits relaxation oscillations, that is, asymmetric oscillations corresponding to slow increase followed by much faster decrease of  $\Delta P_{RD}$ . They corresponds also to intermittent increase and decrease in discharge rate from the central reservoir into the distal storage zone. These transient variations in  $q_{RD}$  produce pressure drops in the central reservoir that, in turn, produce a flow from the lava lake into the central reservoir potentially causing significant lava lake level drops.

### 4.3.2. Period Between Episodes of Lateral Magma Transport and Amplitude of Lava Lake Level Drops

The period between each episode of lateral magma transport into the distal storage zone can be estimated by the following expression:

$$T_R \simeq R^+ \frac{V_R}{E_R} \int_0^{\frac{\bar{q}}{2}} \frac{1 - 2 \frac{q_{RD}}{\bar{q}}}{Q \left(1 + \frac{A_{L,P} E_R}{V_R \rho_m g}\right)^{-1} - q_{RD} \left[\frac{E_D V_R}{V_D E_R} + \left(1 + \frac{A_{L,P} E_R}{V_R \rho_m g}\right)^{-1}\right]} dq_{RD}. \quad (18)$$

This estimation is valid only when  $\tau^* > 1$  and  $R^* \gg 1$  but offers insights on how  $T_R$  depends on the different parameters of our model. The value of  $T_R$  corresponds to the time for the system to build up large enough pressure difference between the central reservoir and the distal storage zone in order for  $\bar{L} = L$  and for the flow resistance  $R_{RD}$  to drop to  $R^-$  inducing an acceleration of  $q_{RD}$ . The duration  $T_R$  scales with  $R^+ \frac{V_R}{E_R}$  and reveals also potential top-down control the lava lake exert on the deeper part of the plumbing system because of  $T_R$  dependence on the cross sectional area of the lava lake that changes significantly from  $A_L$  to  $A_p$  when the lava lake overflows (Figures 3a and 3c). It depends also significantly on the ratio between the quantities  $V_R/E_R$ ,  $V_D/E_D$  and  $A_{L,P}/\rho_m g$  that characterize the storage capacities of the central reservoir, the distal storage zone, and the lava lake respectively (Equation 18 and Figure S1 in Supporting Information S1).

During the phase of pressure build up,  $dq_{RD}/dt = 0$  and the difference of pressure  $\Delta P_{RD}$  that builds up during the time  $T_R$  in between two episodes of lateral magma transport can be estimated simply by:

$$\Delta P_{RD} \simeq \frac{R^+ \bar{q}}{4}. \quad (19)$$

During the phase of lateral magma transport, the pressure gradient that builds up in between the central and distal magma bodies during the time  $T_R$  drops and follows approximately:

$$\Delta P_{RD}(t) \simeq \frac{R^+ \bar{q}}{4} \exp\left(-\frac{t}{\tau_{RL-D}}\right) \quad (20)$$

Here, the time scale characterizing the process is:

$$\tau_{RL-D} = R^- \left(\frac{E_D}{V_D} + \frac{\tau_{RL}}{R_{RL}}\right)^{-1} \quad (21)$$

and corresponds to the characteristic time for the magma both within the lava lake and the reservoir to be drained into the distal storage zone. The resulting amplitude of lava lake level drop is directly proportional to:  $\frac{R^+ \bar{q}}{4}$  and

$$\Delta h_L^{drop} \simeq \frac{\beta}{\rho_m g} \frac{R^+ \bar{q}}{4} \quad (22)$$

with

$$\beta = \frac{E_R}{V_R} \frac{\rho_m g}{A_L} \left( \frac{E_D}{V_D} + \frac{\tau_{RL}}{R_{RL}} \right)^{-1} \left( \frac{E_R}{V_R} + \frac{\rho_m g}{A_{L,P}} \right)^{-1}. \quad (23)$$

## 5. Discussion and Conclusions

All the model's insights provided in Section 4 together with lava lake level measurements can be used to constrain the model's parameters to produce synthetic lava lake level time series capturing features of the observations as in Figure 3a. The lava lake time series provides the following constraints: the linear rate of lava lake increase  $\alpha_L \sim 25$  m/yr Equation 13, the amplitude of lava lake drop  $\Delta h_L^{drop} \sim 10$ –100 m Equation 22, the time in between drops  $T_R \sim 0.2$ –1 year Equation 18, and the drop's characteristic time scale  $\tau_{RL-D} \sim 1$ –3 days Equation 21. Observations of lava lake geometry provide values for the cross sectional area of the lava lake  $A_L \sim 3.10^4$  m<sup>2</sup> and the surrounding platform  $A_p \sim 5.10^5$  m<sup>2</sup> (Barrière et al., 2022; Figure 1d and Figure S2 in Supporting Information S1).

As supported by infrasound and seismic observations, we also assume that the lava lake acts as a piezometer and  $\tau^* = 10$  (Barrière et al., 2018, and Section 4.2). In addition, for the present model to produce lava lake drops level of significant magnitude, the compliance  $V_D/E_D$  of the distal storage zone has to be relatively large, that is,  $V_D/E_D \times (A_P/\rho_m g)^{-1} \geq 1$  and  $V_D E_D \times (V_R/E_R)^{-1} \geq 1$ . For the simulations presented in Figure 3a,  $V_D/E_D \times (A_P/\rho_m g)^{-1} = 1$  and  $V_D E_D \times (V_R/E_R)^{-1} = 10$ .

What emerges also from the model's constraints is that  $R^* \sim 100$ . It means that the flow resistance  $R_{RD}$  has to cover two orders of magnitude during the cycles of reservoir pressure build up and subsequent drop caused by the lateral flow of magma. As the flow resistance is proportional to the fluid viscosity,  $R^* \sim 100$  might be the result of magma viscosity spanning also two orders of magnitude. In that case, variations in magma temperature of hundreds of degrees Celsius can possibly induce the required change in flow resistance (e.g., Morrison et al., 2020; Whitehead & Helfrich, 1991).

All of these above considerations, summarized in Tables S3–S5 in Supporting Information S1, allow to create lava lake simulations as displayed in Figures 3a and 3b and capturing first-order quantitative and qualitative features of the lava lake behavior from 2015 to 2021. The middle time series in Figure 3a shows successive lava lake drops of amplitude  $\Delta h \sim 50$  m spaced by a recovery time of  $T_R \sim 1$  year. This lava lake simulation can directly be compared with the observations represented below on the same Figure and displaying lava lake drops of the same magnitude and sometimes spaced by a period of roughly  $\sim 1$  year.

The simulation displayed in the middle of Figure 3a accounts for overflows. Overflows can significantly slow down the pressure build up within the lava lake in between level drops affecting the recovery time  $T_R$  as illustrated by the comparison between the top and bottom simulated time series in Figure 3a. This highlights an interesting mechanism of top-down control that the lava lake has onto the deeper part of the plumbing system.

Nyiragongo's lava lake level time series in Figure 3a may reflect such a top-down control mechanism as it displays sometimes sharp change in the rate of lava lake level increase when it reaches the rim level and overflows. It occurs clearly in 2018: after the lava lake level drops, it starts to recover at a relatively high rate until it reaches the rim, overflowing, and exhibiting a decrease in the rate of level increase (Figure 1d).

It is also interesting to compare the behavior observed at Nyiragongo with similar ones that occurred at Kilauea's summit lava lake in Hawaii. Between 2010 and 2012 Kilauea lava lake exhibited three level drops of amplitude up to  $\sim 200$  m, spaced by several months and synchronous to eruptive activity in the East Rift Zone (Anderson & Poland, 2016; Patrick et al., 2015; Patrick, Orr, et al., 2019). Insofar they are related to intermittent lateral magma transport, our model may also help to understand the conditions of their occurrence.

Overall, the simple modeling framework developed in this study provides useful insights into the conditions for which deep lateral magma transport causes the observed lava lake level drops. The model can herein be seen as a building block that can be progressively augmented or modified to account for more detailed observations.

For example, one can substitute the lateral flow into the distal storage zone by a flow into a growing intrusion (McLeod & Tait, 1999; Segall et al., 2001). Such a modification is suggested by the NE extension of the deep seismic swarms during each level drop, as well as by the fact that the constitutive earthquakes share characteristics with volcano-tectonic seismic events, both facts pointing to intrusion growth by lateral propagation (Barrière et al., 2019, 2022). While such a change in the model may come at the price of introducing additional unconstrained parameters and variables, it may also help to understand some of the observations unaccounted for by the present model such as the variations in level drops amplitude and recovery time.

## Data Availability Statement

The data set used in this study including the lava lake time series and Nyiragongo's seismicity synchronous to the level drops were previously published and can be accessed through the supplementary of Barrière et al. (2022), (<https://doi.org/10.1029/2021JB023858>).

## References

- Allard, P., Burton, M., Sawyer, G., & Bani, P. (2016). Degassing dynamics of basaltic lava lake at a top-ranking volatile emitter: Ambrym volcano, Vanuatu arc. *Earth and Planetary Science Letters*, *448*, 69–80. <https://doi.org/10.1016/j.epsl.2016.05.014>
- Anderson, K. R., & Poland, M. P. (2016). Bayesian estimation of magma supply, storage, and eruption rates using a multiphysical volcano model: Kilauea Volcano, 2000–2012. *Earth and Planetary Science Letters*, *447*, 161–171. <https://doi.org/10.1016/j.epsl.2016.04.029>
- Barmin, A., Melnik, O., & Sparks, R. (2002). Periodic behavior in lava dome eruptions. *Earth and Planetary Science Letters*, *199*(1–2), 173–184. [https://doi.org/10.1016/s0012-821x\(02\)00557-5](https://doi.org/10.1016/s0012-821x(02)00557-5)
- Barrière, J., d'Oreye, N., Oth, A., Geirsson, H., Mashagiro, N., Johnson, J. B., et al. (2018). Single-station seismo-acoustic monitoring of Nyiragongo's lava lake activity (D.R. Congo). *Frontiers of Earth Science*, *6*, 82. <https://doi.org/10.3389/feart.2018.00082>
- Barrière, J., d'Oreye, N., Oth, A., Theys, N., Mashagiro, N., Subira, J., et al. (2019). Seismicity and outgassing dynamics of Nyiragongo volcano. *Earth and Planetary Science Letters*, *528*, 115821. <https://doi.org/10.1016/j.epsl.2019.115821>
- Barrière, J., d'Oreye, N., Smets, B., Oth, A., Delhaye, L., Subira, J., et al. (2022). Intra-Crater eruption dynamics at Nyiragongo (D.R. Congo), 2002–2021. *Journal of Geophysical Research: Solid Earth*, *127*(4), e2021JB023858. <https://doi.org/10.1029/2021JB023858>
- Batchelor, C. K., & Batchelor, G. (2000). *An introduction to fluid dynamics*. Cambridge university press.
- Bobrowski, N., Giuffrida, G. B., Yalire, M., Lübcke, P., Arellano, S., Balagizi, C., et al. (2017). Multi-component gas emission measurements of the active lava lake of Nyiragongo, DR Congo. *Journal of African Earth Sciences*, *134*, 856–865. <https://doi.org/10.1016/j.jafrearsci.2016.07.010>
- Burgi, P. Y., Boudoire, G., Rufino, F., Karume, K., & Tedesco, D. (2020). Recent activity of Nyiragongo (Democratic Republic of Congo): New insights from field observations and numerical modeling. *Geophysical Research Letters*, *47*(17), e2020GL088484. <https://doi.org/10.1029/2020GL088484>
- Burgi, P. Y., Darrah, T. H., Tedesco, D., & Eymold, W. K. (2014). Dynamics of the mount Nyiragongo lava lake: Dynamics of the Mt. Nyiragongo LAVA LAKE. *Journal of Geophysical Research: Solid Earth*, *119*(5), 4106–4122. <https://doi.org/10.1002/2013JB010895>
- Burgi, P. Y., Minissale, S., Melluso, L., Mahinda, C. K., Cuoco, E., & Tedesco, D. (2018). Models of the formation of the 29 February 2016 new spatter cone inside Mount Nyiragongo. *Journal of Geophysical Research: Solid Earth*, *123*(11), 9469–9485. <https://doi.org/10.1029/2018JB015927>
- Conrad, W. A. (1969). Pressure-flow relationships in collapsible tubes. *IEEE Transactions on Biomedical Engineering*, (4), 284–295. <https://doi.org/10.1109/tbme.1969.4502660>
- Delaney, P. T., & Pollard, D. D. (1982). Solidification of basaltic magma during flow in a dike. *American Journal of Science*, *282*(6), 856–885. <https://doi.org/10.2475/ajs.282.6.856>
- Demant, A., Lestrade, P., Lubala, R. T., Kampunzu, A. B., & Durieux, J. (1994). Volcanological and petrological evolution of Nyiragongo volcano, Virunga volcanic field, Zaire. *Bulletin of Volcanology*, *56*(1), 47–61. <https://doi.org/10.1007/bf00279728>
- Durieux, J. (2002). The pre-2002 activity-volcano Nyiragongo (DR Congo): Evolution of the crater and lava lakes from the discovery to the present (Vol. 1000–1008).
- Harris, A. J., Flynn, L. P., Rothery, D. A., Oppenheimer, C., & Sherman, S. B. (1999). Mass flux measurements at active lava lakes: Implications for magma recycling. *Journal of Geophysical Research*, *104*(B4), 7117–7136. <https://doi.org/10.1029/98jb02731>
- Huppert, H. E., & Woods, A. W. (2002). The role of volatiles in magma chamber dynamics. *Nature*, *420*(6915), 493–495. <https://doi.org/10.1038/nature01211>
- Jordan, D., & Smith, P. (2007). *Nonlinear ordinary differential equations: An introduction for scientists and engineers*. OUP.
- Komorowski, J. C. (2002). The January 2002 eruption—the January 2002 flank eruption of Nyiragongo volcano (democratic Republic of Congo): Chronology, evidence for a tectonic rift trigger, and impact of lava flows on the city of Goma (pp. 1000–1035).
- Le Guern, F. (1987). Mechanism of energy transfer in the lava lake of Niragongo (Zaire), 1959–1977. *Journal of Volcanology and Geothermal Research*, *31*(1–2), 17–31. [https://doi.org/10.1016/0377-0273\(87\)90003-5](https://doi.org/10.1016/0377-0273(87)90003-5)
- Lev, E., Ruprecht, P., Oppenheimer, C., Peters, N., Patrick, M., Hernández, P. A., et al. (2019). A global synthesis of lava lake dynamics. *Journal of Volcanology and Geothermal Research*, *381*, 16–31. <https://doi.org/10.1016/j.jvolgeores.2019.04.010>
- McLeod, P., & Tait, S. (1999). The growth of dykes from magma chambers. *Journal of Volcanology and Geothermal Research*, *92*(3–4), 231–245. [https://doi.org/10.1016/s0377-0273\(99\)00053-0](https://doi.org/10.1016/s0377-0273(99)00053-0)
- Melnik, O., & Sparks, R. (1999). Nonlinear dynamics of lava dome extrusion. *Nature*, *402*(6757), 37–41. <https://doi.org/10.1038/46950>
- Montgomery-Brown, E. K. (2022). *The search for eruption signals in volcanic noise*. Nature Publishing Group.
- Morrison, A. A., Whittington, A., Smets, B., Kervyn, M., & Schlike, A. (2020). The rheology of crystallizing basaltic lavas from Nyiragongo and Nyamuragira volcanoes, DRC. *Volcanica*, *3*(1), 1–28. <https://doi.org/10.30909/vol.03.01.0128>
- Oppenheimer, C., & Kyle, P. R. (2008). Probing the magma plumbing of Erebus volcano, Antarctica, by open-path FTIR spectroscopy of gas emissions. *Journal of Volcanology and Geothermal Research*, *177*(3), 743–754. <https://doi.org/10.1016/j.jvolgeores.2007.08.022>

- Oppenheimer, C., McGonigle, A., Allard, P., Wooster, M., & Tsanev, V. (2004). Sulfur, heat, and magma budget of Erta 'Ale lava lake, Ethiopia. *Geology*, 32(6), 509–512. <https://doi.org/10.1130/g20281.1>
- Oth, A., Barrière, J., d'Oreye, N., Mavonga, G., Subira, J., Mashagiro, N., et al. (2017). KivuSNet: The first dense broadband seismic network for the Kivu Rift Region (Western branch of East African Rift). *Seismological Research Letters*, 88(1), 49–60. <https://doi.org/10.1785/0220160147>
- Patrick, M., Anderson, K. R., Poland, M. P., Orr, T. R., & Swanson, D. A. (2015). Lava lake level as a gauge of magma reservoir pressure and eruptive hazard. *Geology*, 43(9), 831–834. <https://doi.org/10.1130/g36896.1>
- Patrick, M., Orr, T., Anderson, K., & Swanson, D. (2019). Eruptions in sync: Improved constraints on Kilauea volcano's hydraulic connection. *Earth and Planetary Science Letters*, 507, 50–61. <https://doi.org/10.1016/j.epsl.2018.11.030>
- Patrick, M., Orr, T., Sutton, A., Lev, E., Thelen, W., & Fee, D. (2016). Shallowly driven fluctuations in lava lake outgassing (gas pistonning), Kilauea volcano. *Earth and Planetary Science Letters*, 433, 326–338. <https://doi.org/10.1016/j.epsl.2015.10.052>
- Patrick, M., Swanson, D., & Orr, T. (2019). A review of controls on lava lake level: Insights from Halema 'uma 'u crater, Kilauea Volcano. *Bulletin of Volcanology*, 81(3), 1–26. <https://doi.org/10.1007/s00445-019-1268-y>
- Pedley, T. J. (1980). Flow in collapsible tubes. In *The fluid mechanics of large blood vessels* (pp. 301–368). Cambridge University Press. <https://doi.org/10.1017/CBO9780511896996.007>
- Pinel, V., Jaupart, C., & Albino, F. (2010). On the relationship between cycles of eruptive activity and growth of a volcanic edifice. *Journal of Volcanology and Geothermal Research*, 194(4), 150–164. <https://doi.org/10.1016/j.jvolgeores.2010.05.006>
- Reverso, T., Vandemeulebrouck, J., Jouanne, F., Pinel, V., Villemain, T., Sturkell, E., & Bascou, P. (2014). A two-magma chamber model as a source of deformation at Grímsvötn Volcano, Iceland. *Journal of Geophysical Research: Solid Earth*, 119(6), 4666–4683. <https://doi.org/10.1002/2013jb010569>
- Schönfeld, J. C. (1954). Analogy of hydraulic, mechanical, acoustic and electric systems. *Applied Scientific Research, Section A*, 3(1), 417–450. <https://doi.org/10.1007/bf02919918>
- Segall, P., Cervelli, P., Owen, S., Lisowski, M., & Miklius, A. (2001). Constraints on dike propagation from continuous GPS measurements. *Journal of Geophysical Research*, 106(B9), 19301–19317. <https://doi.org/10.1029/2001JB000229>
- Smets, B., d'Oreye, N., Kervyn, M., & Kervyn, F. (2017). Gas piston activity of the Nyiragongo lava lake: First insights from a stereographic time-lapse camera system. *Journal of African Earth Sciences*, 134, 874–887. <https://doi.org/10.1016/j.jafrearsci.2016.04.010>
- Smittarello, D., Smets, B., Barrière, J., Michellier, C., Oth, A., Shreve, T., et al. (2022). Precursor-free eruption triggered by edifice rupture at Nyiragongo volcano. *Nature*, 609(7925), 83–88. <https://doi.org/10.1038/s41586-022-05047-8>
- Tanaka, K. (1983). Seismicity and focal mechanism of the volcanic earthquakes in the Virunga Volcanic region. *Volcanoes Nyiragongo and Nyamuragira: geophysical aspects*, 19–28.
- Tazieff, H. (1977). An exceptional eruption: Mt. Niragongo, Jan. 10 th, 1977. *Bulletin of Volcanology*, 40(3), 189–200. <https://doi.org/10.1007/bf02596999>
- Tazieff, H. (1985). Recent activity at Nyiragongo and lava-lake occurrences. *Geol Soc Finl*, 57(1–2), 11–19. <https://doi.org/10.17741/bgsf/57.1-2.001>
- Tazieff, H. (1994). Permanent lava lakes: Observed facts and induced mechanisms. *Journal of Volcanology and Geothermal Research*, 63(1–2), 3–11. [https://doi.org/10.1016/0377-0273\(94\)90015-9](https://doi.org/10.1016/0377-0273(94)90015-9)
- Van der Pol, B. (1926). Lxxxviii. on “relaxation-oscillations”. *The London, Edinburgh and Dublin Philosophical Magazine and Journal of Science*, 2(11), 978–992. <https://doi.org/10.1080/14786442608564127>
- Walwer, D., Ghil, M., & Calais, E. (2019). Oscillatory nature of the Okmok volcano's deformation. *Earth and Planetary Science Letters*, 506, 76–86. <https://doi.org/10.1016/j.epsl.2018.10.033>
- Walwer, D., Ghil, M., & Calais, E. (2022). A data-based minimal model of episodic inflation events at volcanoes. *Frontiers of Earth Science*, 10, 759475. <https://doi.org/10.3389/feart.2022.759475>
- Wang, T., Zheng, Y., Pulvirenti, F., & Segall, P. (2021). Post-2018 caldera collapse Re-inflation uniquely constrains Kilauea's magmatic system. *Journal of Geophysical Research: Solid Earth*, 126(6), e2021JB021803. <https://doi.org/10.1029/2021JB021803>
- Wauthier, C., Cayol, V., Kervyn, F., & d'Oreye, N. (2012). Magma sources involved in the 2002 Nyiragongo eruption, as inferred from an InSAR analysis. *Journal of Geophysical Research*, 117(B5), B05411. <https://doi.org/10.1029/2011jb008257>
- Whitehead, J., & Helfrich, K. R. (1991). Instability of flow with temperature-dependent viscosity: A model of magma dynamics. *Journal of Geophysical Research*, 96(B3), 4145–4155. <https://doi.org/10.1029/90jb02342>